2014 IEEE International Conference on Robotics & Automation (ICRA)
Hong Kong Convention and Exhibition Center
May 31 - June 7, 2014. Hong Kong, China

Elastodynamic Analysis of Cable-Driven Parallel Manipulators Considering Dynamic Stiffness of Sagging Cables

Han Yuan, Eric Courteille, Dominique Deblaise

Abstract— **This paper focuses on the elastodynamic analysis of cable-driven parallel manipulators. Dynamic stiffness matrix of a single sagging cable is introduced. This matrix considers the effect of both cable mass and elasticity. Dynamic response functions are evaluated for cable-driven parallel manipulators. As an example, the dynamic analysis of a 6-DOF cable-suspended parallel manipulator is achieved considering the dynamic behavior of sagging cables. Numerical simulations and tests are demonstrated to validate the model by identifying the natural frequencies. Effects of cable sag on the static pose error are also experimentally investigated. Results show the importance of taking into consideration the cable dynamics for cable-driven parallel manipulators when it comes to perform applications such as high speed pick-and-place or large working volume.**

I. INTRODUCTION

Cable-driven parallel manipulators (CDPMs) are a special variant of traditional rigid-link parallel manipulators. Using flexible cables rather than rigid links has lots of advantages, such as higher dynamics due to smaller moving mass, much larger workspace, and lower cost. However, as cables present the particularity of not being rigid and are only able to act in tension, the stiffness of CDPMs becomes a vital concern [1], [2]. Effects of cable stiffness are significant for the kinematics analysis, workspace definition, pose accuracy, force distribution, vibration and control of CDPMs [3], [4].

Although stiffness has been well studied in the last few decades for rigid-link parallel manipulators [3]–[8], there is little literature on the stiffness problem of CDPMs. Previous studies mainly consider cables as ideal lines without mass or elasticity [9]–[11].

When it comes to static stiffness analysis, many studies used linear or non-linear spring as the cable model [12]–[20]. This approach considers the elasticity along cable axis and neglects cable mass. Another well known model is the static sagging cable model derived from civil engineering [21]. It is used in several previous researches [1], [2], [22]–[24]. For example: stiffness matrix of a single cable induced by sag is derived, and a sample 3-DOF planar manipulator stiffness is estimated in [22]; Relationship between cable sagging and manipulator stiffness is analyzed through the mapping of intuitive stiffness indices [24]. Generally speaking, sagging cable model considering the effect of mass and elasticity is more accurate than spring cable model in the static stiffness analysis. But sagging model leads to a system with non-linear equations, where cable force and cable length are coupled. Experimental verification of the static characteristics is only performed on a single sagging cable [21], [22] and not on a complete CDPM.

Some applications of CDPM require high performances, especially the dynamic behaviors. For examples: the ultra-high speed FALCON robot [14], [15], the wind-induced vibration problem of the large radio telescope [25]. These applications lead to study cable vibrations and the resulting platform vibrations. Vibrations can be induced by initial position and velocity of the moving platform, wind disturbance, and/or friction of the cables around fixed pulleys [26]. In these situations, dynamic stiffness of cables must be taken into consideration. Manipulator vibrations due to axial and transversal cable flexibilities are studied in [27], and natural frequencies are calculated in [27], [28]. Through a linearization method, the natural frequencies of a 3-DOF planar CDPM are calculated in [22]. Cable model used in [27] and [28] is spring model with elasticity but without mass. Cable mass and flexibility are considered only for the static stiffness computation in [22], but neglected for the system natural frequency computation. As a matter of fact, in many situations, cable mass and elasticity affect system dynamics by changing natural frequencies values and/or adding new resonances.

In this paper, a new dynamic stiffness model is proposed to analyze the vibrations of CDPMs. It is based on the dynamic stiffness matrix of a continuous, flexible, extensible, sagging cable [29]. This matrix considers the effects of both cable mass and elasticity. The dynamic stiffness matrix and dynamic response functions of CDPM are achieved considering the coupling between platform motions and cable-end forces. The effects of cable sag on the static pose error and on the dynamic response functions of a 6-DOF cable-suspended manipulator are numerically and experimentally investigated.

This paper is organized as follows. Dynamic stiffness matrix of a single sagging cable is firstly introduced in Section II. Then dynamic characteristics of CPDM are presented in Section III, including dynamic stiffness matrix deduction and dynamic response functions computation. Section IV presents an example of a 6-DOF cable-suspended manipulator, and discusses the effects of dynamic sagging cable by numerical simulations and experiments. The effects of cable sag on the static pose error are also experimentally investigated. An explicit comparison with the results of other methods available in literature is presented. Finally, conclusions are made in Section V.

Han YUAN, Eric Courteille and Dominique Deblaise are with the Université Européenne de Bretagne, INSA-LGCGM-EA 3913, 20 Avenue des Buttes de Coösmes CS 70839 F-35708 Rennes Cedex 7, France. Corresponding author: Eric Courteille. yuan.han.robot@gmail.com, eric.courteille@insa-rennes.fr, dominique.deblaise@insa-rennes.fr

II. DYNAMIC STIFFNESS MATRIX OF SAGGING CABLE

In this section, improved dynamic stiffness matrix of a single cable is formulated by considering the cable mass, elasticity and damping [29]. The model for an inclined cable is presented in Fig. 1. One of the cable-ends is fixed, and an external force is applied to the other end of the cable. Under the effect of external force and gravity, the shape of the cable between points A and B is not a straight line, but a sagging curve. The cable is considered as a continuum and its shape is given by l (the chord length), d (the sag perpendicular to the chord), and α (the inclination angle). According to [29], the following assumptions are made.

- The cable is assumed to be uniform with unstrained cross section area A, mass per unit length m, and linear Young's modulus E.
- Only small displacements are admitted to meet the requirement of linear theory.
- Out-of-plane cable motion is neglected.
- Only small cable sag is allowed, where the sag to span ratio is no more than 1/20.
- Viscous damping is taken into consideration.

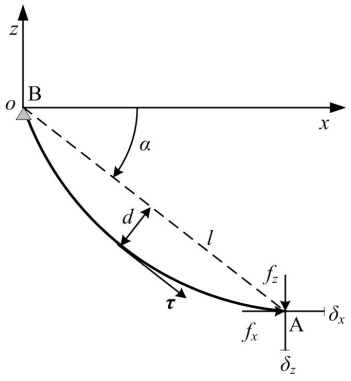

Fig. 1. Diagram of a sagging cable

Derived in a local xyz-coordinate system where the z-axis is vertical, the planar stiffness matrix $\mathbf{K}$ of a single sagging cable can be defined as the relationship between the forces $[f_x, f_z]$ applied at the end point of the cable and the displacements $[\delta_x, \delta_z]$ at the same position (1). The displacement and force are both defined as differentials that represent small changes in position or force from static equilibrium.

$$\begin{bmatrix} f_x \\ f_z \end{bmatrix} = \mathbf{K} \begin{bmatrix} \delta_x \\ \delta_z \end{bmatrix} \tag{1}$$

According to [29], the stiffness matrix $\mathbf{K}$ of a planar sagging cable is a function of τ (the static cable tension at the section where the cable is parallel to the chord), c (the damping force per unit length and velocity), and ω (the frequency of harmonic motion). The expression of $\mathbf{K}$ is given by:

$$\mathbf{K}(\omega) = \begin{bmatrix} K_{11}(\omega) & K_{12}(\omega) \\ K_{21}(\omega) & K_{22}(\omega) \end{bmatrix}, \tag{2}$$

where:

$$K_{11}(\omega) = k_a \cos^2\alpha - 2k_b \sin\alpha\cos\alpha + k_c \sin^2\alpha, \tag{3}$$

$$K_{12}(\omega) = k_a \cos\alpha\sin\alpha - k_b \sin^2\alpha + k_b \cos^2\alpha - k_c \sin\alpha\cos\alpha, \tag{4}$$

$$K_{21}(\omega) = K_{12}, \tag{5}$$

$$K_{22}(\omega) = k_a \sin^2\alpha + 2k_b \sin\alpha\cos\alpha + k_c \cos^2\alpha. \tag{6}$$

The relative parameters in stiffness matrix $\mathbf{K}$ components are:

$$k_a(\omega) = \frac{EA}{L_e} \frac{1}{1 + \frac{\lambda^2}{\Omega_c^2}(\kappa - 1)}, \tag{7}$$

$$k_b(\omega) = \frac{EA}{L_e} \frac{\frac{1}{2}\varepsilon(\kappa - 1)}{1 + \frac{\lambda^2}{\Omega_c^2}(\kappa - 1)}, \tag{8}$$

$$k_c(\omega) = \frac{EA}{L_e}\frac{\varepsilon^2}{\lambda^2}\frac{1}{\kappa} - \frac{EA}{L_e} \frac{\frac{1}{4}\frac{\varepsilon^2}{\lambda^2}\Omega_c^2\left[\kappa + \frac{\lambda^2}{\Omega_c^2}(\kappa - 1)\right]}{1 + \frac{\lambda^2}{\Omega_c^2}(\kappa - 1)}, \tag{9}$$

where:

- $\lambda^2 = \left(\frac{mgl}{\tau}\right)^2 \frac{EAl}{\tau L_e}\cos^2\alpha$ is the fundamental cable parameter which represents the elastic stiffness relative to the catenary stiffness,
- $\varepsilon = \frac{8d}{l}$ is the ratio between horizontal cable weight and cable tension,
- $L_e = \int_0^l \left(\frac{ds}{dx}\right)^3 dx \simeq l\left[1 + 8\left(\frac{d}{l}\right)^2\right]$ is one of the cable parameters,
- $\xi = \frac{c}{2m\omega}$ is the damping ratio,
- $\omega_c = \omega\sqrt{1 - 2\xi i}$ is the frequency-damping parameter,
- $\Omega_c = \omega_c l\sqrt{\frac{m}{\tau}}$ is the dimensionless frequency-damping parameter,
- $\kappa = \frac{\tan\left(\frac{\Omega_c}{2}\right)}{\left(\frac{\Omega_c}{2}\right)}$ is an auxiliary term.

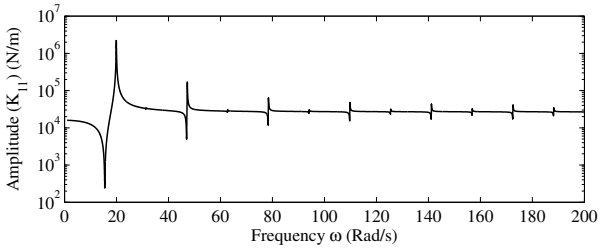

Fig. 2. The amplitude variation of the dynamic stiffness coefficient of an example cable

The dynamic stiffness coefficient $K_{11}(\omega)$ of an example cable is calculated. The cable properties are: $E = 20$ Gpa, $A = 1.2566 \times 10^{-5}$ m^2, $l = 6.848$ m, $\tau = 77.6$ N, $\alpha = 36°$, $\xi = 0.003$. The relevant parameters: $\frac{L_e}{l} = 1.0003 \approx 1$, $\lambda^2 = 7.57$ and $\varepsilon = 0.048$. The amplitude variation of the dynamic stiffness coefficient $K_{11}(\omega)$ is plotted with respect to the frequency of harmonic motion ω in Fig. 2. As one can see, the contribution of the cable vibrations must be considered because considerable variations of the dynamic stiffness amplitude are present within the range of

the natural frequencies, and these variations are associated with symmetric and antisymmetric modes of the cable.

For sake of conciseness, only vibrations within the cable plane are considered here. In linear theory the in-plane motion is uncoupled from the out-of-plane motion. Extension to spatial dynamic stiffness matrix is possible without major difficulty [30].

III. DYNAMIC CHARACTERISTICS OF CDPMS

A. PROBLEM DESCRIPTION

According to the arrangement of the cables, two kinds of CDPMs can be considered. One is cable-suspended parallel manipulator, where all the driven cables are above the moving platform and gravity acts as a virtual cable to keep equilibrium, such as the CoGiRo robot [31]. The other is non-suspended or fully constrained cable parallel manipulator, where at least one driven cable is below the moving platform, such as the FALCON robot [15]. For non-suspended cable parallel manipulators, manipulator stiffness can be reinforced and vibrations can be reduced by increasing cable forces from redundant actuation [15]. In addition, knowledge of modal characteristics of the manipulator is useful to attenuate the wind-induced vibrations (wind-tunnel applications) or to improve the high-speed cable robot control. For cable-suspended parallel manipulator, manipulator stiffness remains broadly lower. In this case, a major control issue is to suppress the platform vibrations to ensure the positioning accuracy by decreasing the stabilization time, such as pick-and-place applications. So inherent dynamic coupling analysis between manipulator motions and dynamic cable stiffness is strongly needed for the two kinds of CDPMs. This section focuses on cable-suspended parallel manipulator but the method can be extended to non-suspended cable parallel manipulators. In this section, the dynamic stiffness matrix of cable-suspended parallel manipulator is established. The dynamic response functions and the natural frequencies are used to investigate its properties.

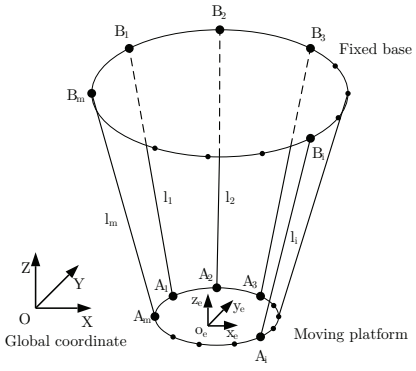

Fig. 3. General configuration of cable-suspended parallel manipulator

Fig. 3 presents a general configuration of cable-suspended parallel manipulator. A_i is the attachment point in the moving platform. B_i is the attachment point in the fixed base. $\Re_G$ (O_G, x, y, z) is the fixed global frame. $\Re_e$ (o_e, x_e, y_e, z_e) is the local frame located on the moving platform. L_i is the length of the i^{th} cable.

B. COMPUTATION OF STIFFNESS MATRIX

Firstly, the dynamic stiffness matrix of each cable $\mathbf{K}_i(\omega)$ (2) should be expressed in the global frame (Fig. 3) as:

$$\mathbf{K}_{Gi}(\omega) = \mathbf{Tr}_i^{-1}\mathbf{K}_i(\omega)\mathbf{Tr}_i, \tag{10}$$

where $\mathbf{Tr}_i$ is the rotation matrix from the i^{th} local cable frame to the global frame. Then the stiffness matrix of the manipulator $\mathbf{K}_M(\omega)$ can be assembled by considering all driven cables:

$$\mathbf{K}_M(\omega) = \sum_{i=1}^{m} \mathbf{A}_i^T \mathbf{K}_{Gi}(\omega)\mathbf{A}_i, \tag{11}$$

where:

$$\mathbf{A}_i = \begin{bmatrix} 1 & 0 & 0 & 0 & -z_{\overrightarrow{o_eA_i}} & y_{\overrightarrow{o_eA_i}} \\ 0 & 1 & 0 & z_{\overrightarrow{o_eA_i}} & 0 & -x_{\overrightarrow{o_eA_i}} \\ 0 & 0 & 1 & -y_{\overrightarrow{o_eA_i}} & x_{\overrightarrow{o_eA_i}} & 0 \end{bmatrix}. \tag{12}$$

Furthermore, the manipulator stiffness matrix can also be expressed as $\mathbf{K}_e(\omega)$ in the platform frame $\Re_e$ (o_e, x_e, y_e, z_e) using the rotation matrix $\mathbf{T}_e$.

C. VIBRATION ANALYSIS

For CDPMs, the system stiffness is mainly affected by the stiffness of their cables, actuators, and moving platform. Compared with cables, the compliance of actuators and moving platform are much lower and therefore neglected. The free vibration equations of a CDPM can be written as:

$$\mathbf{M}\ddot{\bar{\mathbf{x}}}(t) + \mathbf{K}_e(\omega)\bar{\mathbf{x}}(t) = \mathbf{0}, \tag{13}$$

where $\bar{\mathbf{x}}$ represents the perturbation of the moving platform in position and orientation from the static equilibrium. $\mathbf{M}$ is the 6 by 6 mass matrix of the moving platform.

In the previous study [22], [27], [28], cable mass is neglected on the vibration analysis. The system stiffness matrix $\mathbf{K}_e$ is constant. According to the free vibration theory of multi-degree-of-freedom system, the natural frequencies of the CDPM can be calculated by transforming system dynamic equation into its modal space, and then solving the classic eigenvalue and eigenvector problems.

However, in this paper, both cable mass and elasticity are considered. As a result, the system stiffness matrix $\mathbf{K}_e(\omega)$ is function of frequency ω. The above method for linear multi-degree-of-freedom system is not suitable. The analysis of the dynamic response function of the manipulator to a harmonic excitation can be used.

For each pose of the moving platform path, the dynamic equation of a CDPM under a harmonic excitation can be written as:

$$\mathbf{M}\ddot{\bar{\mathbf{x}}}(t) + \mathbf{K}_e(\omega)\bar{\mathbf{x}}(t) = \mathbf{F}e^{j\omega t}. \tag{14}$$

Assuming that the vibration response of the moving platform is $\bar{\mathbf{x}}(t) = \mathbf{X}e^{j\omega t}$, solve (14):

$$\mathbf{X} = \left(-\omega^2\mathbf{M} + \mathbf{K}_e(\omega)\right)^{-1}\mathbf{F}. \tag{15}$$

The dynamic amplification due to resonance will enable to identify the manipulator natural frequencies.

IV. EFFECTS OF SAGGING CABLE ON THE STATIC AND DYNAMIC BEHAVIORS OF THE MANIPULATOR

In this section, a 6-DOF cable-suspended parallel manipulator driven by 6 cables is presented as an example to investigate the effects of sagging cable on the static and dynamic characteristics of CDPM.

A. STUDIED MODEL DESCRIPTION

As presented in Fig. 4, there are 6 attachment points on the three vertical poles and 6 attachment points on the moving platform. These points are connected by 6 cables. This configuration is similar to the prototype presented in [1]. Table I gives the configuration parameters of the 6-DOF CDPM.

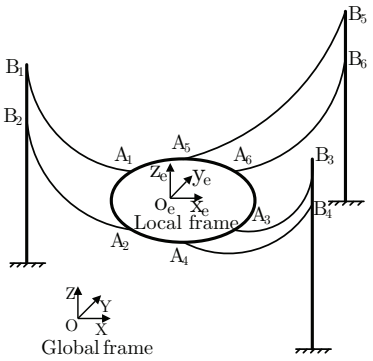

Fig. 4. 6-DOF CDPM example

TABLE I

CONFIGURATION PARAMETERS: COORDINATES OF THE POINTS B_i IN GLOBAL FRAME AND THAT OF A_i IN LOCAL FRAME

(m)	x	y	z		x	y	z
A_1	−0.025	−0.143	0	B_1	5.327	−2.267	4.193
A_2	0.136	−0.050	0	B_2	5.327	−2.267	3.822
A_3	0.136	0.050	0	B_3	5.327	2.267	4.193
A_4	−0.025	0.143	0	B_4	5.327	2.267	3.822
A_5	−0.111	0.093	0	B_5	−5.775	0.010	4.193
A_6	−0.111	−0.093	0	B_6	−5.775	0.010	3.822

B. STATIC PLATFORM POSE ERROR ANALYSIS

The effect of sagging cable on the static behavior of CDPM is firstly considered.

1) Definition of Pose Error: For a traditional rigid-link manipulator, the platform pose error can be defined by its Cartesian stiffness matrix, assuming the compliant displacements of the platform is small [5]. However, as the nonlinearity of sagging cable, the small displacement assumption is not valid. Here direct kinematic model is used to define pose error.

For a given set of unstrained cable lengths l_0, the pose of the platform can be obtained through direct kinematic model. In the modeling of direct kinematics, different cable models can be used, such as ideal cable model where the cable is considered to be inextensible straight line without mass, spring cable model where the cable is simplified as linear spring without mass, and sag cable model where elastic catenary is employed considering both cable mass and elasticity. The difference between the pose obtained through the spring cable model or the sag cable model and the reference pose obtained through the ideal cable model defines the static pose error of the manipulator.

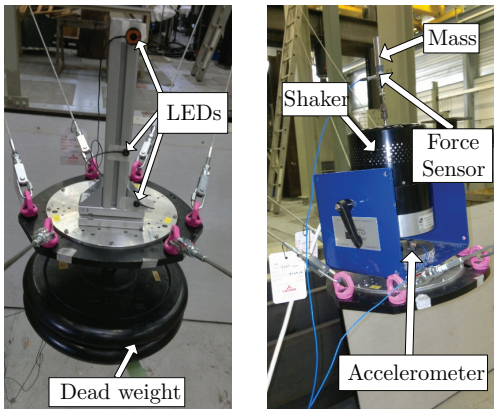

(a) Static experiment (b) Dynamic experiment

Fig. 5. Experimental setup

2) Simulation and Experiment: The experimental setup consists of the 6-DOF cable robot, a precise multi-camera system for tracking the pose of the platform and a loading device connected to the center of the platform. The measurement device is the Nikon Metrology K600-10 system based on three CCD linear cameras and infra-red light active LEDs. Three LEDs are attached to the platform and its poses (both position and orientation) are measured by the camera. The system has a position measuring accuracy up to ± 37 μm for a single point. The mass of the platform can be adjusted from 10.55 kg to 86.35 kg by adding deadweights as shown in Fig. 5(a). Two sets of anti-rust steel cables are used: 4 and 8 mm in diameter. The cable Young's modulus is identified using a material testing machine. All the cables work within their linear elastic region. The relevant cable parameters are given in Table II.

TABLE II

CABLE PARAMETERS

Diameter		4 mm			8 mm		
Length (mm)	$l_{01} \sim l_{03}$	6863	6565	6756	4859	4552	4830
	$l_{04} \sim l_{06}$	6663	6801	6604	4586	9417	9284
Young's Modulus		20 GPa			20 GPa		
Mass per meter		0.067 kg/m			0.251 kg/m		

Fig. 6 shows the effect of platform mass on the static platform pose error along z axis. Firstly, it is showed that the experimental data are quite close to the curve of sag model. These results demonstrate for the first time the validity of the sag cable model on a complete CDPM. When the mass of platform is small, the relationship between mass and

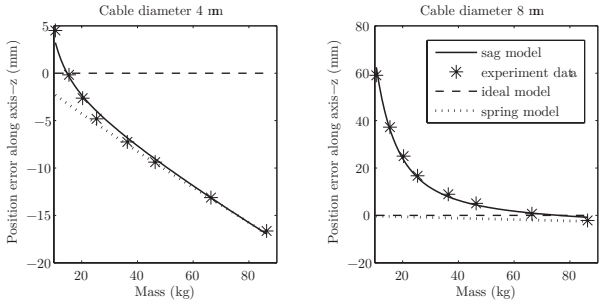

Fig. 6. Effect of platform mass on the static pose error

static pose error is strongly non-linear. This non-linearity is mainly caused by the large cable sag. Beyond a certain threshold value, the non-linearity of sag model becomes much weak, thus both sag model and spring model have a good prediction. These simulations are useful for the design procedure of a CDPM by choosing the mass of platform, the cable parameters and the suitable control model.

C. MANIPULATOR DYNAMIC STIFFNESS ANALYSIS

In order to verify the dynamic stiffness model reliability, tests have been performed to calculate the dynamic response function of the 6-DOF CDPM. As explained before, we consider the dynamic response function plot as the most useful output when dealing with resonance identification for non-linear system. Fig. 5(b) represents the experimental setup, with the platform and an electro-dynamic shaker mounted on it. Experiments have been performed with a stepped sine excitation, i.e. harmonic excitation at a fixed frequency changed step by step (step size: 0.05 Hz) with a stabilization time period of 8 s at each step. The examined frequency range is $1 \sim 20$ Hz because the main interest in suspended cable robot is to consider the first natural frequencies. Over all the examined frequency range, the shaker delivers a vertical force proportional to the acceleration amplitude of the small mass fixed to the mobile device. The presented Frequency Response Function (FRF) in Fig. 7 has been calculated referring to the response of the triaxial accelerometer fixed on the platform and the response of the force sensor. From this amplitude plot it is possible to identify the resonance frequencies. The 6-DOF CDPM exhibits several damped modes in the frequency range studied (Table III). The correlation between experiment results and simulations could be considered more than acceptable referring to the related manipulator natural frequencies values (Fig. 7 and Table III). Obtained results allow to conclude that natural frequencies estimation of CDPM is accurate even critical aspects remain. In fact, as one can see in Fig. 7, the correlation between analytical and experimental FRF in terms of amplitude is not so good and should be explained by presence of noise test data (resonances due to fixture device at low frequencies) and a bad damping estimation. Also, the adopted shaker inertia has been estimated. It could partially explain the differences. The same simulation has been done using the cable model considering out-of-plane motion. But the value of the identified natural frequencies does not change much. The results obtained with the dynamic stiffness model of the CDPM should be compared with the ones obtained with the traditional stiffness models [22], [27], which omit the coupling between the dynamics of the platform and the cable resonances. From the comparison in Table III, it is indicated that the dynamics of the cables change the value of natural frequencies and add new resonances.

TABLE III
NATURAL FREQUENCY COMPARISON AMONG DIFFERENT METHODS

	Manipulator's natural frequencies (range: $0 \sim 10$Hz)											
Experimental data ($\pm$0.1Hz)	1.2	1.5	1.8	2.0	2.5	4.0	4.7	5.6	6.3	7.7	8.6	9.5
Proposed dynamic model	1.1	1.4	1.8	2.0	4.3	4.6	5.4	6.3	7.8	9.4	-	-
Sagging cable model [22]	1.4	2.1	4.6	6.0	7.7	-	-	-	-	-	-	-
Spring cable model [27]	2.8	5.6	8.2	9.5	-	-	-	-	-	-	-	-

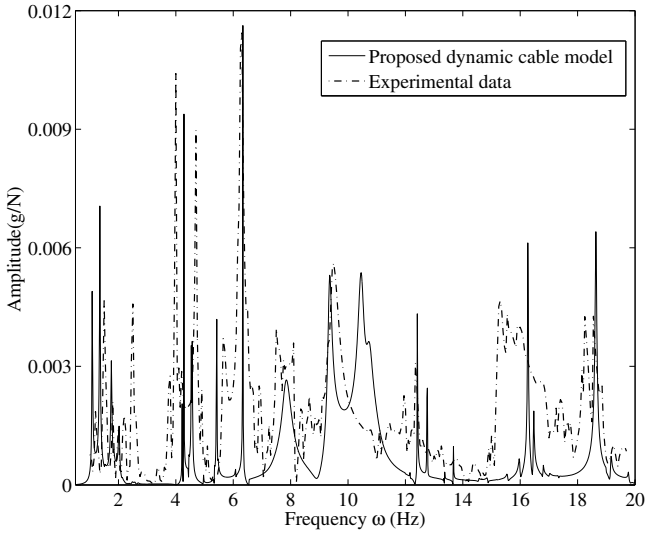

Fig. 7. Frequency response function between the acceleration response of the platform along y-axis and the excitation force along z-axis

V. CONCLUSIONS

This paper focuses on the analysis of the dynamic stiffness matrix of cable-driven manipulators. Dynamic stiffness matrix of a single sagging cable is introduced in order to perform the dynamic characteristics of cable manipulators. Based on this model, dynamic response functions of the manipulator are computed and natural frequencies are identified. The proposed approach has been applied on a 6-DOF cable-suspended parallel manipulator and successfully validated by experiments. A significant correlation between the measured and computed FRF, and the corresponding natural frequency deviations confirm the quality of the model. Results show that cable dynamics has an obvious effect on the manipulator dynamic behavior. Natural frequencies obtained by different

methods available in literature are also compared with the experimental results. Besides dynamic analysis, the effects of different static cable models on the pose error are studied. We demonstrate that Irvine's static sag cable model is necessary to decrease pose error when platform mass is low, and linear spring cable model is enough to guarantee the static accuracy when the platform mass is high. And this threshold value can be found by the proposed method. Further experiments will be performed in order to investigate the damping deeper in detail and actuator stiffness identification.

REFERENCES

[1] M. Gouttefarde, J. Collard, N. Riehl, and C. Baradat, "Simplified static analysis of large-dimension parallel cable-driven robots," in *IEEE International Conference on Robotics and Automation (ICRA)*, pp. 2299 –2305, May 2012.

[2] N. Riehl, M. Gouttefarde, S. Krut, C. Baradat, and F. Pierrot, "Effects of non-negligible cable mass on the static behavior of large workspace cable-driven parallel mechanisms," in *IEEE International Conference on Robotics and Automation (ICRA)*, pp. 2193 –2198, May 2009.

[3] C. Gosselin, "Stiffness mapping for parallel manipulators," *IEEE Transactions on Robotics and Automation*, vol. 6, pp. 377 –382, June 1990.

[4] J.-P. Merlet, *Parallel robots*. Springer, 2006.

[5] G. Carbone, "Stiffness analysis and experimental validation of robotic systems," *Frontiers of Mechanical Engineering*, vol. 6, no. 2, pp. 182–196, 2011.

[6] E. Courteille, D. Deblaise, and P. Maurine, "Design optimization of a delta-like parallel robot through global stiffness performance evaluation," in *IEEE/RSJ International Conference on Intelligent Robots and Systems (IROS)*, pp. 5159 –5166, Oct. 2009.

[7] D. Deblaise, X. Hernot, and P. Maurine, "A systematic analytical method for PKM stiffness matrix calculation," in *IEEE International Conference on Robotics and Automation (ICRA)*, pp. 4213–4219, 2006.

[8] B. S. El-Khasawneh and P. M. Ferreira, "Computation of stiffness and stiffness bounds for parallel link manipulators," *International Journal of Machine Tools and Manufacture*, vol. 39, no. 2, pp. 321 – 342, 1999.

[9] M. Gouttefarde, J.-P. Merlet, and D. Daney, "Wrench-feasible workspace of parallel cable-driven mechanisms," in *IEEE International Conference on Robotics and Automation (ICRA)*, pp. 1492 – 1497, Apr. 2007.

[10] J. Pusey, A. Fattah, S. Agrawal, and E. Messina, "Design and workspace analysis of a 6-6 cable-suspended parallel robot," *Mechanism and Machine Theory*, vol. 39, no. 7, pp. 761 – 778, 2004.

[11] M. Khosravi, H. Taghirad, and R. Oftadeh, "A positive tensions PID controller for a planar cable robot: An experimental study," in *First RSI/ISM International Conference on Robotics and Mechatronics (ICRoM)*, pp. 325–330, 2013.

[12] R. Verhoeven, M. Hiller, and S. Tadokoro, "Workspace, stiffness, singularities and classification of tendon-driven stewart platforms," in *Advances in Robot Kinematics: Analysis and Control*, pp. 105–114, Springer Netherlands, 1998.

[13] N. G. Dagalakis, J. S. Albus, B.-L. Wang, J. Unger, and J. D. Lee, "Stiffness study of a parallel link robot crane for shipbuilding applications," *Journal of Offshore Mechanics and Arctic Engineering*, vol. 111, no. 3, p. 183, 1989.

[14] S. Kawamura, W. Choe, S. Tanaka, and S. Pandian, "Development of an ultrahigh speed robot FALCON using wire drive system," in *IEEE International Conference on Robotics and Automation (ICRA)*, vol. 1, pp. 215 –220 vol.1, May 1995.

[15] S. Kawamura, H. Kino, and C. Won, "High-speed manipulation by using parallel wire-driven robots," *Robotica*, vol. 18, pp. 13–21, Jan. 2000.

[16] S. Behzadipour and A. Khajepour, "Stiffness of cable-based parallel manipulators with application to stability analysis," *Journal of Mechanical Design*, vol. 128, no. 1, p. 303, 2006.

[17] M. Korayem, M. Bamdad, and M. Saadat, "Workspace analysis of cable-suspended robots with elastic cable," in *IEEE International Conference on Robotics and Biomimetics (ROBIO)*, pp. 1942–1947, Dec. 2007.

[18] Y. Bedoustani, H. Taghirad, and M. Aref, "Dynamics analysis of a redundant parallel manipulator driven by elastic cables," in *10th International Conference on Control, Automation, Robotics and Vision (ICARCV)*, pp. 536–542, Dec. 2008.

[19] A. Vafaei, M. Khosravi, and H. Taghirad, "Modeling and control of cable driven parallel manipulators with elastic cables: Singular perturbation theory," in *Intelligent Robotics and Applications* (S. Jeschke, H. Liu, and D. Schilberg, eds.), vol. 7101 of *Lecture Notes in Computer Science*, pp. 455–464, Springer Berlin / Heidelberg, 2011.

[20] M. A. Khosravi and H. D. Taghirad, "Robust PID control of cable-driven robots with elastic cables," in *First RSI/ISM International Conference on Robotics and Mechatronics (ICRoM)*, pp. 331–336, 2013.

[21] H. M. Irvine, *Cable structures*. Dover Publications, 1992.

[22] K. Kozak, Q. Zhou, and J. Wang, "Static analysis of cable-driven manipulators with non-negligible cable mass," *IEEE Transactions on Robotics*, vol. 22, pp. 425 – 433, June 2006.

[23] J. Sandretto, G. Trombettoni, and D. Daney, "Confirmation of hypothesis on cable properties for cable-driven robots," in *New Trends in Mechanism and Machine Science* (F. Viadero and M. Ceccarelli, eds.), vol. 7 of *Mechanisms and Machine Science*, pp. 85–93, Springer Netherlands, 2013.

[24] M. Arsenault, "Workspace and stiffness analysis of a three-degree-of-freedom spatial cable-suspended parallel mechanism while considering cable mass," *Mechanism and Machine Theory*, vol. 66, pp. 1–13, Aug. 2013.

[25] B. Zi, B. Duan, J. Du, and H. Bao, "Dynamic modeling and active control of a cable-suspended parallel robot," *Mechatronics*, vol. 18, pp. 1–12, Feb. 2008.

[26] J. Du, H. Bao, C. Cui, and D. Yang, "Dynamic analysis of cable-driven parallel manipulators with time-varying cable lengths," *Finite Elements in Analysis and Design*, vol. 48, pp. 1392–1399, Jan. 2012.

[27] X. Diao and O. Ma, "Vibration analysis of cable-driven parallel manipulators," *Multibody System Dynamics*, vol. 21, pp. 347–360, May 2009.

[28] O. Ma and X. Diao, "Dynamics analysis of a cable-driven parallel manipulator for hardware-in-the-loop dynamic simulation," in *IEEE/ASME International Conference on Advanced Intelligent Mechatronics (AIM)*, pp. 837 –842, July 2005.

[29] U. Starossek, "Dynamic stiffness matrix of sagging cable," *Journal of Engineering Mechanics*, vol. 117, pp. 2815–2828, Dec. 1991.

[30] J. Kim and S. P. Chang, "Dynamic stiffness matrix of an inclined cable," *Engineering Structures*, vol. 23, pp. 1614–1621, Dec. 2001.

[31] T. Dallej, M. Gouttefarde, N. Andreff, R. Dahmouche, and P. Martinet, "Vision-based modeling and control of large-dimension cable-driven parallel robots," in *IEEE/RSJ International Conference on Intelligent Robots and Systems (IROS)*, pp. 1581 –1586, Oct. 2012.